

## Tailoring Site Specificity of Bioconjugation using Step-Wise ATRP on Proteins (SWAP)

Sheiliza Carmali, Hironobu Murata, Krzysztof Matyjaszewski, and Alan J Russell

*Biomacromolecules*, Just Accepted Manuscript • DOI: 10.1021/acs.biomac.8b01064 • Publication Date (Web): 06 Sep 2018

Downloaded from <http://pubs.acs.org> on September 13, 2018

### Just Accepted

“Just Accepted” manuscripts have been peer-reviewed and accepted for publication. They are posted online prior to technical editing, formatting for publication and author proofing. The American Chemical Society provides “Just Accepted” as a service to the research community to expedite the dissemination of scientific material as soon as possible after acceptance. “Just Accepted” manuscripts appear in full in PDF format accompanied by an HTML abstract. “Just Accepted” manuscripts have been fully peer reviewed, but should not be considered the official version of record. They are citable by the Digital Object Identifier (DOI®). “Just Accepted” is an optional service offered to authors. Therefore, the “Just Accepted” Web site may not include all articles that will be published in the journal. After a manuscript is technically edited and formatted, it will be removed from the “Just Accepted” Web site and published as an ASAP article. Note that technical editing may introduce minor changes to the manuscript text and/or graphics which could affect content, and all legal disclaimers and ethical guidelines that apply to the journal pertain. ACS cannot be held responsible for errors or consequences arising from the use of information contained in these “Just Accepted” manuscripts.

# Tailoring Site Specificity of Bioconjugation using Step-Wise ATRP on Proteins (SWAP)

*Sheiliza Carmali<sup>1,2</sup>, Hironobu Murata<sup>1</sup>, Krzysztof Matyjaszewski<sup>1,2</sup>, Alan J. Russell<sup>1,2,3,\*</sup>*

<sup>1</sup>Center for Polymer-Based Protein Engineering, Carnegie Mellon University, 5000 Forbes Avenue, Pittsburgh, Pennsylvania, 15213 United States

<sup>2</sup>Department of Chemistry, Carnegie Mellon University, 5000 Forbes Avenue, Pittsburgh, Pennsylvania, 15213 United States

<sup>3</sup>Department of Chemical Engineering, Carnegie Mellon University, 5000 Forbes Avenue, Pittsburgh, Pennsylvania, 15213 United States

## KEYWORDS

Protein-ATRP, initiator, inhibitor, bioconjugates, step-wise, site-specific

1  
2  
3  
4 ABSTRACT  
5

6 Protein-polymer conjugates are powerful combinations of the biotic and abiotic worlds that  
7 impact many industries. Predicting the site and impact of polymer growth from the surface of  
8 proteins are only useful if we can use that information to choose which site to modify  
9 synthetically. We have explored the combination of a predictive algorithm with a unique step-  
10 wise atom transfer radical polymerization to selectively move the predominant modification sites  
11 around a model enzyme. Lysozyme was modified with defined stoichiometric ratios of  
12 polymerization initiators and initiation inhibitors to selectively and strategically grow poly-  
13 (carboxybetaine methacrylate) polymers from different protein sites. Electrospray ionization  
14 mass spectrometry was used to examine the uniformity of the lysozyme-initiator and lysozyme-  
15 inhibitor complexes prior to polymer growth. Bioactivity of the lysozyme-polymer conjugates  
16 was examined as a function of polymer location on the enzyme surface. Step-wise atom transfer  
17 radical polymerization from proteins provides a versatile and modular approach that can be  
18 extended to the rational and selective design of other protein-polymer conjugates.  
19  
20  
21  
22  
23  
24  
25  
26  
27  
28  
29  
30  
31  
32  
33  
34  
35  
36  
37  
38  
39  
40  
41  
42  
43  
44  
45  
46  
47  
48  
49  
50  
51  
52  
53  
54  
55  
56  
57  
58  
59  
60

## INTRODUCTION

Over the last four decades, protein-polymer conjugates have found applications in research laboratories, industrial facilities and medical clinics<sup>1,2</sup>. The modification of proteins with polymers yields exciting biomacromolecular systems that exhibit properties from both individual components. The function of the bioconjugates depends on the nature, size and location of the polymer on the protein surface. Early work with protein-polymer conjugates relied on the use of poly(ethylene glycol) (PEG) to impart greater stability, solubility and decrease the immune response of proteins<sup>3,4</sup>. Recent advances in the field of protein-polymer chemistry have led to the predictable modification and enhancement of enzyme structure and function under non-native conditions. Researchers<sup>5,6,15,7-14</sup>, including ourselves, have exploited the use of stimuli-responsive polymers for the preparation of bioconjugates with increased pH and temperature stability, increased substrate affinity and stability in non-aqueous conditions.

Despite these numerous benefits and exponential increase in applications, challenges remain in the rational design of bioconjugates. Indeed, the site(s) of modification and number of polymer chains bound to the protein surface have a direct impact on protein function<sup>16-19</sup>. A significant reduction or complete loss in biological function can occur upon modification, particularly when the polymer is located close to the active center<sup>20</sup>. Thus, a delicate balance of polymer distribution on the protein surface is pivotal for optimal protein function. A complete understanding requires knowledge of the conjugation site(s) on the protein surface; the conjugation strategy; the nature of the polymer; protein and polymer conformations during and after modification; and the degree of intra- and intermolecular interaction between polymer and protein. Traditional structure determination methodologies are not always suitable because of the

1  
2  
3 intrinsic complexity and size of these bioconjugates<sup>21-24</sup>. Additionally, protein modification often  
4  
5 results in conjugates with high levels of heterogeneity<sup>22</sup>.  
6

7  
8 One approach to generate more uniformly defined protein-polymer conjugates with high  
9  
10 grafting densities, when desired, is surface-initiated atom-transfer radical polymerization  
11  
12 (ATRP)<sup>10,25</sup>. Using amine-reactive chemistry, small molecule initiators are coupled onto a  
13  
14 protein surface, from where ATRP is used to grow polymers, in situ. ATRP reaction conditions  
15  
16 can be fine-tuned to obtain desired polymer chain lengths at a controlled density. Elegant,  
17  
18 though time consuming, genetic techniques that introduce non-natural amino-acid ATRP  
19  
20 initiators have been used to target polymers to specific sites<sup>26</sup>. In addition, a variety of  
21  
22 chemistries have been introduced to grow polymers from single sites on the protein<sup>11,12</sup>.  
23  
24 Unfortunately, however, there has remained a need for a straightforward way to influence the site  
25  
26 of modification or to protect a desired location from ATRP.  
27  
28  
29

30  
31 We recently used the tertiary structure of proteins to predict the outcome of protein-  
32  
33 ATRP<sup>27</sup>. Our technique enabled us to predict where and how fast ATRP initiators react with  
34  
35 proteins. Knowing the speed and location of ATRP initiator reactions encouraged us to design a  
36  
37 synthetic strategy through which we could use this information to target particular reaction sites.  
38  
39 We decided to take a model protein, lysozyme, use the algorithmic predictions of modification  
40  
41 rate at each available reaction site and then synthetically switch off fast reacting sites and target  
42  
43 selective growth at slow reacting sites. We synthesized a protein-reactive “ATRP-inhibitor” that  
44  
45 was structurally similar to our ATRP initiator. The initiation inhibitor, that lacked the halogen  
46  
47 atom required for initiation of ATRP reactions, was designed to react with amine groups (N-  
48  
49 terminal and lysine side chains) on proteins by N-hydroxysuccinimide chemistry. We  
50  
51  
52  
53  
54  
55  
56  
57  
58  
59  
60

1  
2  
3 hypothesized that the strategic step-wise use of the initiator and inhibitor would lead to tailored  
4  
5 polymer distributions on the surface of lysozyme.  
6

7  
8 Herein, we describe Step-Wise ATRP on Proteins (SWAP) with lysozyme. Lysozyme is  
9  
10 an antimicrobial enzyme and an important component of the innate immune system that has been  
11  
12 widely used for protein conjugation, has a well characterized amine-ATRP initiator reactivity  
13  
14 pattern and a method for evaluating bioactivity<sup>28-30</sup>. These features provide lysozyme with ideal  
15  
16 characteristics to explore the potential of SWAP and the implications of polymer distribution on  
17  
18 protein function. Amine-ATRP initiator and amine-initiation inhibitor reactivities were first  
19  
20 predicted by tertiary structure analysis. The site(s) of modification for both active esters were  
21  
22 confirmed experimentally by enzymatic digestion studies followed by peptide mass mapping.  
23  
24 With a defined reactivity pattern for lysozyme, we attempted three general approaches to  
25  
26 strategic polymer growth (Figure 1). For the modification of the fast-reacting groups in  
27  
28 lysozyme, a stoichiometric approach of ATRP initiator was used. To modify slow-reacting amine  
29  
30 groups, lysozyme was first reacted with a defined stoichiometric amine-to-inhibitor ratio  
31  
32 followed by the addition of excess ATRP initiator. Lastly, to inhibit polymer growth at an amine  
33  
34 group with intermediate reactivity, a multi-step addition ATRP initiator and initiation inhibitor  
35  
36 was used. Electrospray ionization (ESI-MS) and matrix-assisted laser desorption/ionization time-  
37  
38 of-flight mass spectrometry (MALDI-ToF-MS) were used to probe the uniformity of the  
39  
40 lysozyme-initiator and -inhibitor complexes. After poly-(carboxybetaine methacrylate)  
41  
42 (pCBMA) growth by ATRP, the bioactivity of the family of SWAP lysozyme-polymer  
43  
44 conjugates was measured using a *M. lysodeikticus* cell wall degradation assay. This is, to the best  
45  
46 of our knowledge, the first step-wise ATRP approach towards controlled polymer distribution on  
47  
48  
49  
50  
51  
52  
53  
54  
55  
56  
57  
58  
59  
60

proteins. The versatility and ease of SWAP allows for this methodology to be applied to other protein-polymer conjugates.

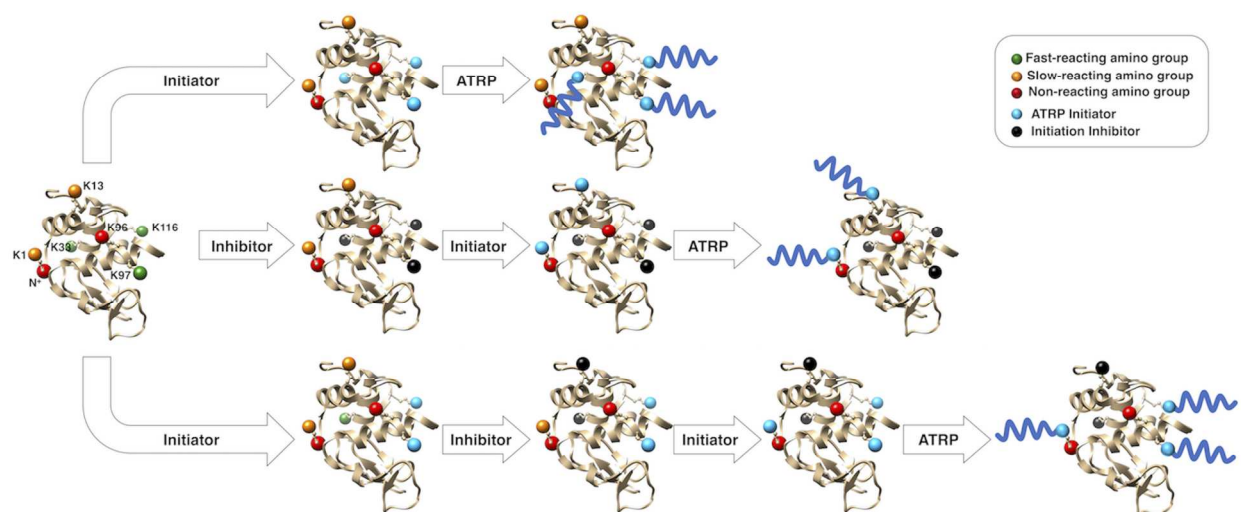


**Figure 1.** Step-Wise ATRP for Proteins (SWAP) for tailored polymer distribution on the surface of lysozyme. Fast-, slow- and non-reacting amine groups (shown in green, orange and red, respectively) are first determined using a tertiary structure based prediction algorithm. Spheres in blue indicate amino groups modified with ATRP initiator while those in black denote amino groups with initiation inhibitors.

## EXPERIMENTAL SECTION

### Materials.

Hen egg-white lysozyme (Lyz) from *Gallus gallus* and lyophilized *Micrococcus lysodeikticus* were purchased from Sigma-Aldrich (St Louis, MO) and used without further purification. Carboxybetaine methacrylate was purchased from TCI America. Bromine-functionalized N-hydroxysuccinimide ATRP initiator **1** synthesis was carried out as described previously<sup>10</sup>. Dialysis tubing (molecular weight cut off 15 kDa Spectra/Por, Spectrum Laboratories Inc., CA) for macro-initiator and macro-inhibitor isolation, ZipTipsC<sub>18</sub> microtips (Millipore, catalogue no. ZTC1 8M0 08), and In-Solution Tryptic Digestion and Guanidination Kits (catalogue no. 89895) were purchased from Thermo Fisher Scientific (Pittsburgh, PA).

## Methods.

### Synthesis of N-isobutyryl- $\beta$ -alanine N'-oxysuccinimide ester **2**.

Isobutyryl chloride (10.5 mL, 100 mmol) was slowly added into a solution of  $\beta$ -alanine (8.9 g, 100 mmol) and triethylamine (30.7 mL, 220 mmol) in mixture of deionized water (100 mL) at 0 °C. The mixture was stirred at room temperature for 1 h. The water phase was washed with diethyl ether (50 mL x 3) and adjusted to pH 2 with 6 N HCl aq. at 0 °C. The product was extracted with ethyl acetate (50 mL  $\times$  5). The organic phase was dried with MgSO<sub>4</sub> and evaporated to remove solvent. N-isobutyryl- $\beta$ -alanine was isolated by recrystallization from a mixture of ethyl acetate and diethyl ether (1:1 volume ratio); yield 9.2 g (58 %), mp 100 – 102 °C. <sup>1</sup>H NMR (300 MHz, CDCl<sub>3</sub>)  $\delta$  1.14 (d, 3 H,  $J$  = 6.9 Hz, NHC=OCH(CH<sub>3</sub>)<sub>2</sub>), 2.36 (m, 1 H,  $J$  = 6.9 Hz, NHC=OCH(CH<sub>3</sub>)<sub>2</sub>), 2.59 (t, 2 H,  $J$  = 6.0 Hz, HOOCCH<sub>2</sub>CH<sub>2</sub>NHC=O), 3.52 (q, 2 H,  $J$  = 6.0 Hz, HOOCCH<sub>2</sub>CH<sub>2</sub>NHC=O), and 6.18 (broad s, 1 H, amide proton) ppm. IR (KBr) 3385, 2970, 2927, 1713, 1632, 1614, 1553, 1435, 1372, 1355, 1307, 1278, 1223, 1199 and 1127 cm<sup>-1</sup>.

N,N'-diisopropylcarbodiimide (3.4 mL, 22 mmol) was slowly added to the solution of N-isobutyryl- $\beta$ -alanine (3.2 g, 20 mmol) and N-hydroxysuccinimide (2.5 g, 22 mmol) in dichloromethane (100 mL) at 0 °C. The mixture was stirred at room temperature overnight. After filtration, the solution was evaporated to remove solvent. N-isobutyryl- $\beta$ -alanine N'-oxysuccinimide ester **2** was purified by recrystallization from 2-propanol with a yield of 4.1 g (80 %), mp 128 – 131 °C. <sup>1</sup>H NMR (300 MHz, CDCl<sub>3</sub>)  $\delta$  1.13 (d, 3 H,  $J$  = 6.9 Hz, NHC=OCH(CH<sub>3</sub>)<sub>2</sub>), 2.37 (m, 1 H,  $J$  = 6.9 Hz, NHC=OCH(CH<sub>3</sub>)<sub>2</sub>), 2.86 and 2.82 (s and t, 4 H and 2 H,  $J$  = 6.0 Hz, ethylene of succinimide and NHSOOCCH<sub>2</sub>CH<sub>2</sub>NHC=O), 3.65 (q, 2 H,  $J$  = 6.0 Hz, NHSOOCCH<sub>2</sub>CH<sub>2</sub>NHC=O), and 6.26 (broad s, 1 H, amide proton). IR (KBr) 3304, 2969, 2876, 1816, 1709, 1741, 1649, 1551, 1428, 1381, 1366, 1310, 1247, 1208 and 1087 cm<sup>-1</sup>.

1  
2  
3 HRMS (m/z):  $[M+Na]^+$  calcd. for  $C_{11}H_{16}N_2O_5$ , 279.09; found 278.93;  $[M+2ACN+H]^+$  calcd. for  
4  $C_{11}H_{16}N_2O_5$ , 339.17; found 338.20.  
5  
6

### 7 **Stoichiometric Reaction between ATRP initiator 1 and Lyz.**

8  
9  
10 A family of lysozyme macro-initiators with varying degrees of modification was prepared using  
11 bromine-functionalized ATRP initiator 1. ATRP initiator 1 (1.6–24.6 mg, 0.005–0.07 mmol) and  
12 Lyz (50 mg, 0.004 mmol protein, 0.02 mmol  $NH_2$  group in lysine residues and N-terminus) were  
13 dissolved in 10 mL of 0.1 M sodium phosphate buffer, pH 8.0. The solution was stirred at 4 °C  
14 for 2 h. After this time, the reaction was dialyzed against deionized water, using dialysis tubing  
15 with a molecular weight cutoff of 15 kDa, for 24 h at 4 °C, and then lyophilized.  
16  
17  
18  
19  
20  
21  
22  
23

### 24 **Reaction between initiator inhibitor 2 and Lyz.**

25  
26 A family of lysozyme macro-inhibitors with varying degrees of modification was prepared using  
27 initiator inhibitor 2. Initiator inhibitor 2 (1.25–12.5 mg, 0.005–0.05 mmol) and Lyz (50 mg,  
28 0.004 mmol protein, 0.02 mmol  $-NH_2$  group in lysine residues and N-terminus) were dissolved in  
29 10 mL of 0.1 M sodium phosphate buffer, pH 8.0. The solution was stirred at 4 °C for 2 h. After  
30 this time, the reaction was dialyzed against deionized water, using dialysis tubing with a  
31 molecular weight cutoff of 15 kDa, for 24 h at 4 °C, and then lyophilized.  
32  
33  
34  
35  
36  
37  
38  
39

### 40 **Synthesis of LyzBr<sub>2</sub>I<sub>1</sub>Br<sub>3</sub>.**

41  
42 Lysozyme (50 mg, 0.0035 mmol protein, 0.024 mmol  $-NH_2$  group in lysine residues and N-  
43 terminus) and ATRP initiator 1 (2.5 mg, 0.007 mmol) were dissolved in 10 mL of 0.1 M sodium  
44 phosphate buffer, pH 8.0. The solution was stirred at 4°C for 30 minutes. After this time, initiator  
45 inhibitor 2 (1.8 mg, 0.007 mmol) was added to the reaction mixture and the solution was stirred  
46 for an additional 30 minutes at 4°C. Lastly, excess ATRP initiator 1 (24.6 mg, 0.07 mmol) was  
47 added to the lysozyme solution and the reaction was stirred for 1 hour. After the total time of 2  
48  
49  
50  
51  
52  
53  
54  
55  
56  
57  
58  
59  
60

1  
2  
3 hours, the reaction was terminated and dialyzed against deionized water, using dialysis tubing  
4  
5 with a molecular weight cutoff of 8 kDa, for 24 h at 4 °C, followed by lyophilization.  
6

#### 7 **ATRP from the surface of Lysozyme.**

8  
9  
10 ATRP was carried out as previously described<sup>31</sup>. In brief, a solution of CBMA and protein-  
11  
12 initiator in 100 mM sodium phosphate, pH 8.0 (for a final concentration of protein-initiator of  
13  
14 0.5 mM) was sealed and bubbled with nitrogen gas for 30 min. 1 mL of deoxygenated catalyst  
15  
16 solution (described below) was then added to the polymerization reactor under bubbling  
17  
18 nitrogen. The mixture was sealed and stirred at room temperature for 2 h. The conjugate was  
19  
20 isolated by dialysis with a 25 kDa molecular weight cutoff dialysis tube in deionized water in a  
21  
22 refrigerator for 24 h and then lyophilized. Note: Approximate final concentrations in solution:  
23  
24 Initiator = 0.5 mM, CuII = 5 mM, NaAsc = 0.5 mM and HMTETA = 6 mM.  
25  
26  
27

#### 28 **Preparation of Cu-HMTETA as deoxygenated catalyst solution.**

29  
30 50 mM CuCl<sub>2</sub> in deionized water (1.2 mL, 60 μmol) was bubbled with N<sub>2</sub> for 25 min and then  
31  
32 100 mM sodium ascorbate in deionized water (50 μL, 5 μmol) was added. HMTETA (18 μL, 70  
33  
34 μmol) was added to the copper suspension bubbled with N<sub>2</sub> for 3 min. The deoxygenated Cu-  
35  
36 HMTETA solution was added to the synthesis vessel immediately.  
37  
38

#### 39 **Lysozyme Activity Assay.**

40  
41  
42 Lysozyme activity was measured by the lysis of *M. lysodeikticus* cell walls as previously  
43  
44 described<sup>32</sup>. Lyophilized *Micrococcus lysodeikticus* was used to monitor enzymatic catalysis of  
45  
46 cell wall lysis. Absorption at 450 nm of suspended *M. lysodeikticus* (990 μL, 0.2 mg/mL) in 50  
47  
48 mM phosphate buffer (pH 6.0) was measured by UV-VIS spectrometer. 10 μL of Lyz-pCBMA  
49  
50 solution (2.8 μM in 50 mM phosphate buffer (pH 6.0)) was added and the change of absorbance  
51  
52 at 450 nm at room temperature was monitored.  
53  
54  
55  
56  
57  
58  
59  
60

### **Determination of Modification Site.**

Trypsin digests were used to generate peptide fragments from which lysozyme macro-inhibitor attachment sites could be determined using ElectroSpray Ionization (ESI) Mass Spectrometry. Samples were digested per the protocol described in the In-Solution Tryptic Digestion and Guanidination Kit. In brief, 20  $\mu\text{g}$  of lysozyme or lysozyme macro-inhibitors (10  $\mu\text{L}$  of a 2 mg/mL protein solution in ultrapure water) were added to 15  $\mu\text{L}$  of 50 mM ammonium bicarbonate with 1.5  $\mu\text{L}$  of 100 mM dithiothreitol (DTT) in a 0.5 mL Eppendorf tube. The reaction was incubated for 5 min at 95  $^{\circ}\text{C}$ . Thiol alkylation was conducted by the addition of 3  $\mu\text{L}$  of 100 mM iodoacetamide aqueous solution to the protein solution and incubation in the dark for 20 min at room temperature. After this time, 1  $\mu\text{L}$  of 100 ng of trypsin was added to the protein solution, and the reaction was incubated at 37  $^{\circ}\text{C}$  for 3 h. An additional 1  $\mu\text{L}$  of 100 ng of trypsin was subsequently added. Digested samples were purified using ZipTip $\text{C}_{18}$  microtips and eluted with 1  $\mu\text{L}$  of 50% acetonitrile with 0.1% formic acid into a 0.5 mL Eppendorf tube and diluted 100-fold with 50% acetonitrile with 0.1% formic acid. The molecular weight of the expected peptide fragments before and after blocking agent attachment was predicted using PeptideCutter (ExpASY Bioinformatics Portal, Swiss Institute of Bioinformatics). A complete list of identified tryptic peptides can be found in supporting information.

### **$^1\text{H}$ NMR spectroscopy.**

$^1\text{H}$  NMR spectra were recorded on a spectrometer (300 MHz Bruker Avance $\text{TM}$  300) in the NMR facility located in Center for Molecular Analysis, Carnegie Mellon University, Pittsburgh, PA, with  $\text{CDCl}_3$ .

### **Fourier-Transform Infrared Analysis.**

1  
2  
3 Routine FT-IR spectra were obtained with a Nicolet Magna-IR 560 spectrometer (Thermo), in  
4 the Department of Chemical Engineering at Carnegie Mellon University.  
5  
6

### 7 **Melting points.**

8  
9  
10 Melting points (mp) were measured with a Laboratory Devices Mel-Temp.  
11

### 12 **MALDI-ToF-MS Analysis.**

13  
14 Matrix assisted laser desorption ionization time-of-flight mass spectrometry (MALDI-TOF MS)  
15 measurements were recorded using a PerSeptive Voyager STR MS with nitrogen laser (337 nm)  
16 and 20 kV accelerating voltage with a grid voltage of 90%. At least 300 laser shots covering the  
17 complete spot were accumulated for each spectrum. For the determination of the molecular  
18 weight of synthesized lysozyme complexes, sinapinic acid (20 mg/mL) in 50% acetonitrile with  
19 0.1% trifluoroacetic acid was used as matrix. Protein solution (1.0 mg/mL) was mixed with an  
20 equal volume of matrix, and 2  $\mu$ L of the resulting mixture was loaded onto a silver sterling plate  
21 target. Apomyoglobin, cytochrome C, and aldolase were used as calibration samples. The extent  
22 of modification was determined by subtracting the lysozyme complexes' m/z values from the  
23 protein lysozyme m/z and dividing by the molecular weight of the ATRP initiator or initiator  
24 inhibitor (220.9 or 142.18 g/mol, respectively).  
25  
26  
27  
28  
29  
30  
31  
32  
33  
34  
35  
36  
37  
38  
39

### 40 **ESI-MS Analysis.**

41  
42 Experiments were performed by using a Finnigan LCQ (Thermo-Fisher) quadrupole field ion  
43 trap mass spectrometer with electrospray ionization (ESI) source. Each scan was acquired over  
44 the range m/z 150-2000 by using a step of 0.5 u, a dwell time of 1.5 ms, a mass defect of 50 pu,  
45 and an 80-V orifice potential. Samples at a protein concentration of 50  $\mu$ M and eluted using 50%  
46 acetonitrile and 0.1% formic acid at a flow rate of 20  $\mu$ L/min.  
47  
48  
49  
50  
51  
52  
53

### 54 **Dynamic Light Scattering (DLS).**

1  
2  
3 The DLS data were collected on a Nanoplus Zeta/Nano Particle Analyzer (Particulate Systems).  
4  
5 The concentration of the sample solution was kept at 1.0 mg/mL. Hydrodynamic diameters ( $D_h$ )  
6  
7 of native lysozyme and conjugates were measured three times (25 runs/measurement) in 100 mM  
8  
9 sodium phosphate buffer (pH 8.0) at 25 °C.  
10

### 11 **Bicinchonic Assay (BCA).**

12  
13  
14 Sample solution in deionized water (25  $\mu$ L, 1.0 mg/mL) was mixed with mixture of bicinchonic  
15  
16 acid (BCA) solution (1.0 mL) and copper (II) sulfate solution (50:1 vol:vol). The sample solution  
17  
18 was incubated at 60 °C for 15 min. Absorbance of the sample at 562 nm was recorded by UV-  
19  
20 VIS spectrometer. Lysozyme concentration (wt%) of the conjugates was determined by  
21  
22 comparison of the absorbance to the standard curve. Standard curve was obtained from native  
23  
24 Lysozyme with different concentration ratio in deionized water. Estimation of molecular weight  
25  
26 for lysozyme-polymer conjugates was determined as previously described<sup>33</sup>.  
27  
28  
29  
30  
31  
32

## 33 RESULTS AND DISCUSSION

34  
35 Lysozyme contains seven amine groups; one  $\alpha$ -amino group of N-terminal (K1) and the six  $\epsilon$ -  
36  
37 amino groups of the lysine residues (K1, K13, K33, K96, K97, and K116)<sup>34,35</sup>. Previous analysis  
38  
39 of the structural and chemical environment surrounding these amine groups allowed us to  
40  
41 determine the occurrence and sequence of amine modifications with ATRP initiator **1**<sup>27</sup>. We  
42  
43 hypothesized that the distinct reactivities of the amine groups in lysozyme could be used to target  
44  
45 modification and tailor polymer growth using the SWAP synthetic strategy (Figure 1).  
46  
47  
48  
49  
50

### 51 **Structure-Reactivity Characterization of the Amine-Initiation Inhibitor Reaction**

To aid in the selectivity and precision of amine modifications, initiation inhibitor **2** was synthesized and characterized by  $^1\text{H-NMR}$  and ESI-MS. Initiation inhibitor **2** was designed to be comparable to the ATRP initiator **1** in terms of structure and reactivity, but prevent polymer growth by ATRP. Thus, the N-hydroxysuccinimide ester group allowed the reaction with lysine residues and N-termini while the absence of a halogen atom prevented polymer growth at this site.

We exposed lysozyme to increasing amounts of initiation inhibitor **2** in 0.1 M sodium phosphate buffer, pH 8, at 4 °C for 2 h to generate a small family of macro-inhibitors (Lyz-I). As a comparison, a family of macro-initiators (Lyz-Br) was also prepared under the same stoichiometric and reaction conditions. We were interested in confirming whether the ATRP initiator **1** and initiation inhibitor **2** would react with the same rate and selectivity with the amine groups in lysozyme. Lysozyme macro-initiators and macro-inhibitors were purified by dialysis and analyzed by MALDI-TOF (Supporting information, Figures S1 and S2).

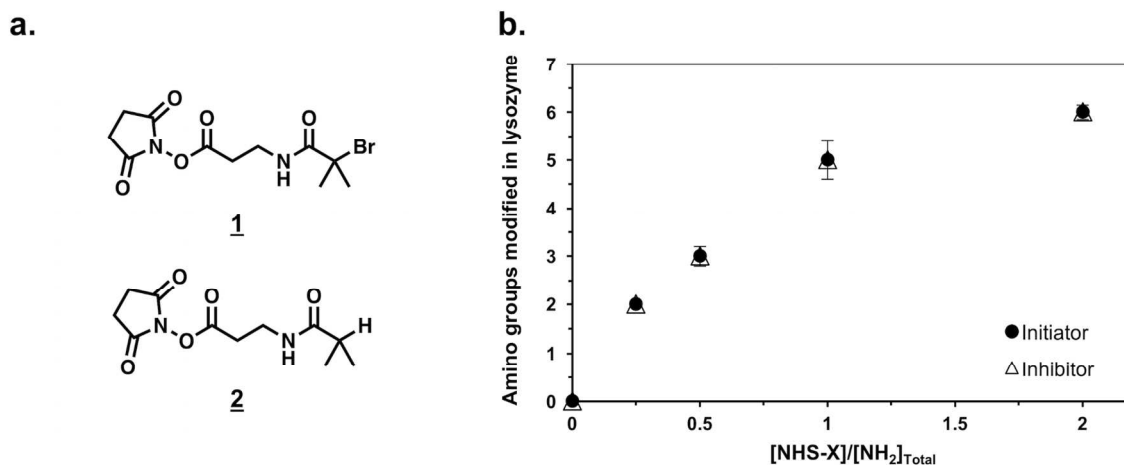


**Figure 2.** Dependence of ATRP initiator **1** versus initiation inhibitor **2** reacting with the surface of lysozyme as a function of the initiator or inhibitor to the amino groups' stoichiometry. Experimentally, native lysozyme was incubated with increasing amounts of ATRP initiator **1** or

1  
2  
3 inhibitor 2 in 0.1 M sodium phosphate buffer, pH 8.0, at room temperature for 2 hours. After this  
4 time, the lysozyme complexes were purified by dialysis and analyzed by MALDI-TOF to  
5 determine the number of amino groups modified. In plot, [NHS-X] represents the concentration  
6 of ATRP initiator 1 or inhibitor 2.  
7  
8  
9

10 The number of initiators in each lysozyme complex was calculated by subtracting native  
11 lysozyme m/z from the Lyz-Br or Lyz-I m/z values and dividing by the molar mass of ATRP  
12 initiator 1 or initiation inhibitor 2 (Mw = 220.9 g/mol or 142.0 g/mol, respectively). As  
13 anticipated, the number of initiator or inhibitor molecules on lysozyme increased when  
14 increasing molar excess of the respective active ester. Moreover, MALDI-ToF analysis indicated  
15 that, on average, both active esters reacted similarly with the amine groups. We were now  
16 interested in determining where initiation inhibitor 2 reacted with the surface of lysozyme.  
17  
18  
19  
20  
21  
22  
23  
24  
25

26 The location of the amine groups that were modified by initiation inhibitors were  
27 identified by trypsin digestion followed by mass spectrometry analysis (see supporting  
28 information, Tables S2 and S3) as described in detail previously<sup>27</sup>. Lysozyme contains six lysine  
29 residues that may be cleaved by trypsin. Previous studies<sup>27,36-38</sup> have shown that the order of  
30 amine modification in lysozyme with ATRP initiator 1 was K116, K97 ~ K33, K13, and finally  
31 K1. Furthermore, we also observed that K96 was non-reactive. MS analysis on the tryptic digests  
32 for the various Lysozyme macro-inhibitors showed that this order of modification was  
33 maintained, indicating identical reactivities between both initiator and inhibitor. Interestingly, an  
34 additional modification was identified on K1 for lysozyme macro-inhibitor (LyzI<sub>6</sub>), suggesting  
35 that two modifications on the same lysine residue were possible ( $\epsilon$ -amino side chain and the N-  
36 terminus). This was not observed previously for lysozyme macro-initiators<sup>27</sup> and was attributed  
37 to steric impediment and low surface exposure of the N-terminus, which would prevent  
38 modification at this site. To further understand this finding, a short 20 ns molecular dynamics  
39  
40  
41  
42  
43  
44  
45  
46  
47  
48  
49  
50  
51  
52  
53  
54  
55  
56  
57  
58  
59  
60

1  
2  
3 simulation was performed on the lysozyme macro-inhibitor with one modification at the  $\epsilon$ -amino  
4 group on K1 and compared to native lysozyme as well as lysozyme macro-initiator also with one  
5  
6 modification at the  $\epsilon$ -amino group on K1 (see supplementary information, Figure S3). End-to-  
7  
8 end distances between the  $\alpha$ - and  $\epsilon$ -amino groups were measured over the simulation time and a  
9  
10 greater distance between both amino groups was observed when K1 was modified with initiation  
11  
12 inhibitor **2**. We inferred that the absence of the bromine atom in the inhibitor molecule decreased  
13  
14 the steric impediment previously seen with ATRP initiator **1**.  
15  
16  
17  
18

19  
20 To further confirm the specificity of amine modifications with both active esters, excess  
21  
22 ATRP initiator **1** was added to LyzI<sub>2</sub> (modified with inhibitor at K116 and K97). Subsequent  
23  
24 MS analysis of trypsin digestion of peptide fragments revealed the initiator now reacted first with  
25  
26 K33, K13 and K1 (see supporting information, Figure S4). Thus, in a SWAP process we could  
27  
28 block the growth of polymer from the most reactive lysine residues.  
29  
30  
31  
32

### 33 **Structural Characterization of Lyz Macro-Initiators and -Inhibitors**

34  
35  
36 In our approach to surface-initiated ATRP, we target modifications at lysine residues and N-  
37  
38 terminus in proteins. Due to the high natural abundance and nucleophilicity of the  $\alpha$ - and  $\epsilon$ -  
39  
40 amino groups, this strategy ensures dense modification to produce nanoarmored enzymes.  
41  
42 However, when more selective modifications are needed, this high abundance of nucleophiles  
43  
44 could yield a statistical population of many products with variable biological outcomes<sup>39-41</sup>. Such  
45  
46 heterogeneity has been observed in early research with first-generation PEGylated products<sup>39</sup>,  
47  
48 but has not been the focus of extensive research with protein-ATRP. We next looked to assess  
49  
50 the promise that site-specific polymer growth synthetic strategies could yield more homogeneous  
51  
52 conjugates with retained and predictable biological effects<sup>42-44</sup>.  
53  
54  
55  
56  
57  
58  
59  
60

1  
2  
3 To examine the uniformity of lysozyme macro-initiators and macro-inhibitors, we  
4 initially performed MALDI-ToF-MS analysis. MALDI-ToF mass signals for macromolecules  
5 correspond to the convolution of the intrinsic isotope distribution. Thus, for lysozyme complexes  
6 (and proteins in general), we observed an envelope of masses due to the distribution of  $^{13}\text{C}$   
7 isotope. This translated visually into a broad spectrum where we assumed that the actual mass  
8 was at the center of the envelope. This value corresponded to the weighted average of all isotope  
9 peaks. Unfortunately, this average mass was not sufficiently precise to develop a real insight into  
10 any heterogeneity of the macro-initiators and macro-inhibitors. To obtain more detailed  
11 structural information on the uniformity of the lysozyme complexes, we developed an ESI-MS  
12 technique with the bioconjugates.  
13  
14  
15  
16  
17  
18  
19  
20  
21  
22  
23  
24  
25

26 ESI-MS is a powerful tool for investigating the covalent modification of proteins with  
27 small molecules. The use of this technique leads to spectra with multiply charged ions allowing  
28 the detection of large proteins using mass analyzers with low mass-to-charge ( $m/z$ ) ranges.  
29 Moreover, the overall mass accuracy and precision of ESI-MS allows low abundance molecules  
30 with small mass differences to be efficiently detected. This can be particularly advantageous  
31 when determining the stoichiometry and uniformity of protein-initiator or protein-inhibitor  
32 complexes.  
33  
34  
35  
36  
37  
38  
39  
40  
41

42 ESI-MS analyses of lysozyme covalently modified with 0.5 and 2.0 equivalents of  
43 initiator inhibitor **2** confirmed the formation of lysozyme macro-inhibitors (**Error! Reference**  
44 **source not found.**c and d). Upon reaction of lysozyme with 0.5 equivalents of initiator inhibitor  
45 **2**, by MALDI analysis we detected the presence of three initiator inhibitors on each protein  
46 molecule (Figure 2b). When analyzed by ESI-MS, we detected a family of products varying in  
47 inhibitor content from one to four per molecule of enzyme (Figure 3c). For lysozyme that was  
48  
49  
50  
51  
52  
53  
54  
55  
56  
57  
58  
59  
60

reacted with molar excess of initiation inhibitor **2**, two distinct populations were identified by ESI-MS (Figure 3d).

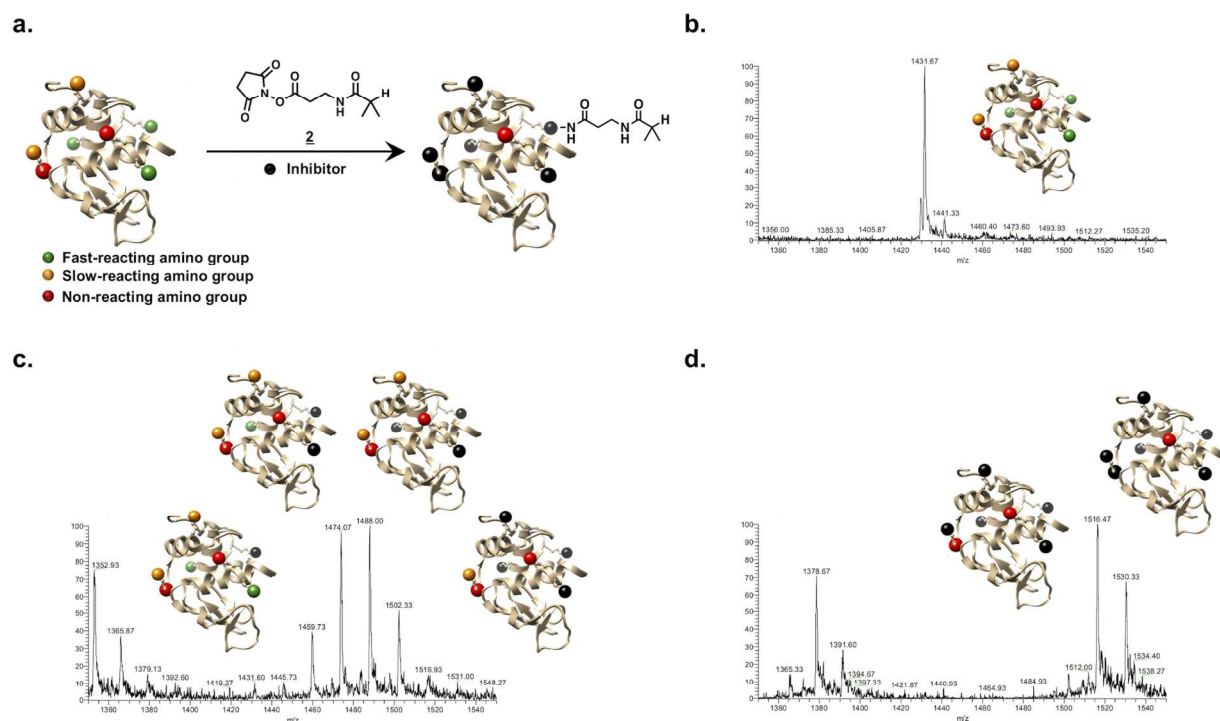


**Figure 3 a.** Initiation inhibitor reaction with lysozyme. Fast, slow and non-reacting amine groups on lysozyme are depicted in green, orange and red, respectively. Amine groups modified with initiation inhibitor **2** are represented in black. ESI-MS spectrum for **b.** native lysozyme, **c.** lysozyme macro-inhibitor with 1-4 inhibitors and **d.** lysozyme macro-initiator with 5-6 ATRP inhibitors. Spectra range shows protein at  $[M+10]^{10+}$  charge state.

The sensitivity of ESI-MS compared to MALDI allowed us to fully understand the uniformity of the starting materials for protein ATRP. When reacted with excess ATRP initiator **1**, lysozyme-initiator complexes with 3 to 5 initiators per molecule of enzyme were observed (see supporting information, Figure S5). Because of the natural abundance of bromine isotopes, the mass spectra resolution was found to decrease dramatically with increasing initiator modification.

## Tailored Polymer Growth by Surface-Initiated ATRP

To test our hypothesis that Step-Wise ATRP on Proteins could be used to tailored polymer distribution, we next grew pCBMA from the initiating sites of the previously prepared lysozyme macro-initiators. Since we were interested in controlling polymer growth to specific locations on the surface of the protein, we maintained the ATRP reaction conditions to obtain similar polymer chain lengths. The protein content for each conjugate was determined by the bicinchoninic acid assay (BCA) which allowed us to determine the apparent molecular weight and degree of pCBMA polymerization (DP) for each of the lysozyme-pCBMA conjugates (Table 1). As the number of polymer chains on the protein surface increased, the overall conjugate molecular weight increased.

**Table 1.** SWAP Synthesis of Active Lysozyme-pCBMA Conjugates. The nomenclature for the lysozyme- conjugates includes the number of ATRP initiators or initiation inhibitors and the determined DP. For example, Lyz-(pCBMA<sub>11</sub>-Br)<sub>2</sub> refers to lysozyme-pCBMA conjugate with two bromine initiators and a DP of 11. The degree of the polymeric carboxybetaine was controlled by maintaining constant the initial molar concentration of the CBMA monomer in solution, which was reflected in the similar DP values for all lysozyme conjugates. The protein content for each conjugate was determined by bicinchoninic acid assay (BCA), from which the apparent molecular weight and DP for each conjugate were calculated. The hydrodynamic diameter values ( $D_h$ ) were determined using dynamic light scattering (DLS) in 100 mM sodium phosphate at pH 8.0. For native lysozyme, the diameter was consistent with that reported in the literature<sup>45</sup>.

	Inhibited -NH <sub>2</sub>	Initiated -NH <sub>2</sub>	DP	Conjugate Mw (Da)	$D_h$ (nm)	<i>M. lysodeikticus</i>	
						$\Delta A_{450}/\text{min}$ ( $\times 10^{-5}$ )	Ratio of lysis (Conjugate/Native)
Native Lysozyme					$3.2 \pm 0.7$	$56.7 \pm 5.8$	$1.00 \pm 0.0$
Lyz-(pCBMA <sub>11</sub> -Br) <sub>2</sub>	-	K116, K97	11	19,235.25	$3.6 \pm 0.7$	$23.3 \pm 5.8$	$0.41 \pm 0.08$

1							
2							
3			K116,				
4		-	K97, K33,	9	22,174.62	4.2 ± 1.0	5.7 ± 1.2
5	Lyz-(pCBMA <sub>9</sub> -Br) <sub>4</sub>		K13				0.10 ± 0.03
6							
7			K116,				
8		-	K97, K33,	13	32,235.25	4.1 ± 1.2	0.9 ± 0.2
9	Lyz-(pCBMA <sub>13</sub> -Br) <sub>6</sub>		K13, K1,				0.02 ± 0.00
10			N <sup>+</sup>				
11							
12	LyzI <sub>2</sub> -(pCBMA <sub>12</sub> -Br) <sub>2</sub>		K33, K13	12	19,883.58	3.1 ± 0.7	20.0 ± 0.0
13							
14			K33, K13,	9	22,477.09	4.0 ± 0.8	1.6 ± 1.2
15	LyzI <sub>2</sub> -(pCBMA <sub>9</sub> -Br) <sub>3</sub>	K116,	K1				0.03 ± 0.02
16		K97					
17			K33, K13,	15	28,472.60	4.6 ± 0.9	1.9 ± 1.1
18	LyzI <sub>2</sub> -(pCBMA <sub>15</sub> -Br) <sub>4</sub>		K1, N <sup>+</sup>				0.03 ± 0.02
19							
20							
21							
22		K33	K116,	13	29,142.76	4.1 ± 0.9	2.3 ± 0.6
23	LyzI <sub>1</sub> -(pCBMA <sub>13</sub> -Br) <sub>5</sub>		K97, K13,				0.04 ± 0.02
24			K1, N <sup>+</sup>				
25							
26							
27							

28 The bioactivity of the family of polymer protein conjugates was assayed in a cell wall  
 29 hydrolysis assay. At physiological pH Lysozyme has a net positive charge, while *Micrococcus*  
 30 *lysodeikticus*, like most other bacterial cells, has a negatively charged outer surface<sup>46</sup>. We  
 31 attributed the decrease in activity of the lysozyme conjugates (when compared to native  
 32 lysozyme) to differences in surface charge of the conjugate, steric impediment of the catalytic  
 33 site to large substrates by the polymers or a combination of the two. Considering the importance  
 34 of the difference in charge between the enzyme and the substrate in this lytic assay, we were not  
 35 surprised to observe the dependence of activity decrease on increasing initiator and pCBMA  
 36 coverage of the enzyme. The activity of lysozyme was inversely proportional to the number of  
 37 polymer chains attached (Table 1 and Figure S6 in supporting information). The active site of  
 38 lysozyme consists of a cleft on the exterior of the enzyme in which only two residues (Glu 35  
 39 and Asp 52) are involved in the catalytic action<sup>47</sup>. The lysine residue that was closest to the  
 40  
 41  
 42  
 43  
 44  
 45  
 46  
 47  
 48  
 49  
 50  
 51  
 52  
 53  
 54  
 55  
 56  
 57  
 58  
 59  
 60

1  
2  
3 active site cleft, Lys 33, was not close enough, however, to eliminate activity when conjugated to  
4  
5 a polymer chain.  
6

7  
8 Previous studies have reported that lysozyme interacts with a negative surface using its  
9  
10 largest positively charged patch, which includes Lys 1, Lys 13, Lys 96, Lys 97, Arg 14 and Arg  
11  
12 128. We were not surprised, therefore, to note that Lyz-(pCBMA<sub>9</sub>-Br)<sub>4</sub> (in which Lys 116, Lys  
13  
14 97, Lys 33 and Lys 13 were modified with pCBMA), had a more pronounced activity reduction  
15  
16 when compared, for example, to LyzI<sub>2</sub>-(pCBMA<sub>12</sub>-Br)<sub>2</sub> (in which only Lys 33 and Lys 13 were  
17  
18 modified with pCBMA). Our results demonstrated that we could engineer lysozyme-pCBMA  
19  
20 conjugates in which polymer chains were grown by SWAP from targeted locations, thereby  
21  
22 rationally tailoring the activity of the enzyme.  
23  
24  
25  
26  
27

## 28 CONCLUSIONS

29  
30 We have used SWAP to synthesize lysozyme-pCBMA conjugates at sites targeted by a  
31  
32 knowledge of lysine reactivity and enzyme structure-function relationships. ATRP initiators and  
33  
34 initiation inhibitors were used in a modular approach to tailor the polymer distribution on the  
35  
36 surface of lysozyme. Macro-initiators and macro-inhibitors were characterized by mass  
37  
38 spectrometry techniques. ESI-MS proved to be a powerful and insightful tool to characterize the  
39  
40 uniformity of the prepared macro-initiators and macro-inhibitors. Structural and mechanistic  
41  
42 insights allowed us to engineer enzyme variants that minimized the loss of critical protein  
43  
44 surface charges (at Lys 97, Lys 33 and Lys 13). When combined with algorithms that can predict  
45  
46 where and how fast individual sites react with ATRP initiators, SWAP can be used to selectively  
47  
48 tailor polymer distribution on the surface of enzymes. We are now exploring the use of SWAP  
49  
50  
51  
52  
53  
54  
55  
56  
57  
58  
59  
60

1  
2  
3 with a range of proteins that require site-selectivity when being subject to grown-from protein-  
4  
5 ATRP.  
6  
7  
8  
9

## 10 SUPPORTING INFORMATION

11  
12 Molecular dynamics simulation study of native lysozyme, lysozyme macro-initiator and  
13  
14 lysozyme macro-inhibitor; MALDI-TOF spectra for the characterization of lysozyme-initiator  
15  
16 and lysozyme-inhibitor complexes; data for the trypsin digestion studies; ESI-MS spectra  
17  
18 characterization for lysozyme-initiator complexes.  
19  
20  
21

## 22 AUTHOR INFORMATION

### 23 24 25 **Corresponding Author**

26  
27  
28 \* Fax: 412-268-5229. E-mail: alanrussell@cmu.edu.  
29  
30

### 31 **Author Contributions**

32  
33  
34 S.C. predicted amine reactivity of lysozyme, prepared lysozyme-initiators and lysozyme-  
35  
36 inhibitors, performed the trypsin digestion studies and analyzed MS data. H.M. synthesized  
37  
38 initiator inhibitor. A.R and K.M supervised the project and provided guidance. The manuscript  
39  
40 was written through contributions of all authors. All authors have given approval to the final  
41  
42 version of the manuscript.  
43  
44  
45

### 46 **Notes**

47  
48  
49 The authors declare no competing financial interest.  
50  
51

## 52 ACKNOWLEDGMENTS

53  
54  
55  
56  
57  
58  
59  
60

The authors acknowledge the financial support provided by the Carnegie Mellon University Center for Polymer-based Protein Engineering.

## REFERENCES

- (1) Wu, Y.; Ng, D. Y. W.; Kuana, S. L.; Weil, T. Protein–polymer Therapeutics: A Macromolecular Perspective. *Biomater. Sci.* **2015**, *3* (2), 214–230.
- (2) Pelegri-O’Day, E. M.; Lin, E.-W.; Maynard, H. D. Therapeutic Protein–Polymer Conjugates: Advancing Beyond PEGylation. *J. Am. Chem. Soc.* **2014**, *136* (41), 14323–14332.
- (3) Veronese, F. M.; Pasut, G. PEGylation, Successful Approach to Drug Delivery. *Drug Discov. Today* **2005**, *10* (21), 1451–1458.
- (4) Veronese, F. M.; Mero, A. The Impact of PEGylation on Biological Therapies. *BioDrugs* **2008**, *22* (5), 315–329.
- (5) Jiang, L.; Bonde, J. S.; Ye, L. Temperature and PH Controlled Self-Assembly of a Protein–Polymer Biohybrid. *Macromol. Chem. Phys.* **2018**, *219* (7), 1–7.
- (6) Kovaliov, M.; Allegranza, M. L.; Richter, B.; Konkolewicz, D.; Averick, S. Synthesis of Lipase Polymer Hybrids with Retained or Enhanced Activity Using the Grafting-from Strategy. *Polymer (Guildf)*. **2018**, *137*, 338–345.
- (7) Cummings, C. S.; Fein, K.; Murata, H.; Ball, R. L.; Russell, A. J.; Whitehead, K. A. ATRP-Grown Protein-Polymer Conjugates Containing Phenylpiperazine Selectively Enhance Transepithelial Protein Transport. *J. Control. Release* **2017**, *255*, 270–278.
- (8) Cummings, C. S.; Murata, H.; Matyjaszewski, K.; Russell, A. J. Polymer-Based Protein Engineering Enables Molecular Dissolution of Chymotrypsin in Acetonitrile. *ACS Macro Lett.* **2016**, *5* (4), 493–497.

- 1  
2  
3 (9) Cummings, C.; Murata, H.; Koepsel, R.; Russell, A. J. Tailoring Enzyme Activity and  
4 Stability Using Polymer-Based Protein Engineering. *Biomaterials* **2013**, *34* (30), 7437–  
5 7443.  
6  
7  
8  
9  
10 (10) Murata, H.; Cummings, C. S.; Koepsel, R. R.; Russell, A. J. Polymer-Based Protein  
11 Engineering Can Rationally Tune Enzyme Activity, PH-Dependence, and Stability.  
12 *Biomacromolecules* **2013**, *14* (6), 1919–1926.  
13  
14  
15  
16  
17 (11) Qi, Y.; Amiram, M.; Gao, W.; McCafferty, D. G.; Chilkoti, A. Sortase-Catalyzed Initiator  
18 Attachment Enables High Yield Growth of a Stealth Polymer from the C Terminus of a  
19 Protein. *Macromol. Rapid Commun.* **2013**, *34* (15), 1256–1260.  
20  
21  
22  
23  
24 (12) Gao, W.; Liu, W.; Mackay, J. A.; Zalutsky, M. R.; Toone, E. J.; Chilkoti, A. In Situ  
25 Growth of a Stoichiometric PEG-like Conjugate at a Protein’s N-Terminus with  
26 Significantly Improved Pharmacokinetics. *Proc. Natl. Acad. Sci. U. S. A.* **2009**, *106* (36),  
27 15231–15236.  
28  
29  
30  
31  
32  
33 (13) Nicolas, J.; Miguel, V. S.; Mantovani, G.; Haddleton, D. M. Fluorescently Tagged  
34 Polymer Bioconjugates from Protein Derived Macroinitiators. *Chem. Commun.* **2006**, *0*  
35 (45), 4697.  
36  
37  
38  
39  
40 (14) Heredia, K. L.; Bontempo, D.; Ly, T.; Byers, J. T.; Halstenberg, S.; Maynard, H. D. In  
41 Situ Preparation of Protein - “Smart” Polymer Conjugates with Retention of Bioactivity. *J.*  
42 *Am. Chem. Soc.* **2005**, *127* (48), 16955–16960.  
43  
44  
45  
46  
47 (15) Lele, B. S.; Murata, H.; Matyjaszewski, K.; Russell, A. J. Synthesis of Uniform Protein-  
48 Polymer Conjugates. *Biomacromolecules* **2005**, *6* (6), 3380–3387.  
49  
50  
51 (16) Perry, J. L.; Reuter, K. G.; Kai, M. P.; Herlihy, K. P.; Jones, S. W.; Luft, J. C.; Napier, M.;  
52 Bear, J. E.; Desimone, J. M. PEGylated PRINT Nanoparticles: The Impact of PEG  
53  
54  
55  
56  
57  
58  
59  
60

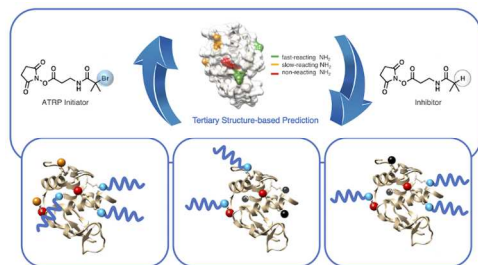
- 1  
2  
3 Density on Protein Binding, Macrophage Association, Biodistribution, and  
4  
5 Pharmacokinetics. *Nano Lett.* **2012**, *12* (10), 5304–5310.  
6  
7  
8 (17) Cobo, I.; Li, M.; Sumerlin, B. S.; Perrier, S. Smart Hybrid Materials by Conjugation of  
9  
10 Responsive Polymers to Biomacromolecules. *Nat. Mater.* **2015**, *14* (2), 143–149.  
11  
12 (18) Pandey, B. K.; Smith, M. S.; Torgerson, C.; Lawrence, P. B.; Matthews, S. S.; Watkins,  
13  
14 E.; Groves, M. L.; Prigozhin, M. B.; Price, J. L. Impact of Site-Specific PEGylation on the  
15  
16 Conformational Stability and Folding Rate of the Pin WW Domain Depends Strongly on  
17  
18 PEG Oligomer Length. *Bioconjug. Chem.* **2013**, *24* (5), 796–802.  
19  
20  
21 (19) Schulz, J. D.; Patt, M.; Basler, S.; Kries, H.; Hilvert, D.; Gauthier, M. A.; Leroux, J. C.  
22  
23 Site-Specific Polymer Conjugation Stabilizes Therapeutic Enzymes in the Gastrointestinal  
24  
25 Tract. *Adv. Mater.* **2016**, *28* (7), 1455–1460.  
26  
27  
28 (20) Wenck, K.; Koch, S.; Renner, C.; Sun, W.; Schrader, T. A Noncovalent Switch for  
29  
30 Lysozyme. *J. Am. Chem. Soc.* **2007**, *129* (51), 16015–16019.  
31  
32  
33 (21) Williams, C.; Dougherty, M. L.; Makaroff, K.; Stapleton, J.; Konkolewicz, D.; Berberich,  
34  
35 J. A.; Page, R. C. Strategies for Biophysical Characterization of Protein– Polymer  
36  
37 Conjugates. *NanoArmoring Enzym. Ration. Des. Polym. Enzym.* **2017**, *590*, 93–114.  
38  
39  
40 (22) Abzalimov, R. R.; Frimpong, A.; Kaltashov, I. A. Structural Characterization of Protein-  
41  
42 Polymer Conjugates. I. Assessing Heterogeneity of a Small PEGylated Protein and  
43  
44 Mapping Conjugation Sites Using Ion Exchange Chromatography and Top-down Tandem  
45  
46 Mass Spectrometry. *Int. J. Mass Spectrom.* **2012**, *312*, 135–143.  
47  
48  
49 (23) Gerislioglu, S.; Adams, S. R.; Wesdemiotis, C. Characterization of Singly and Multiply  
50  
51 PEGylated Insulin Isomers by Reversed-Phase Ultra-Performance Liquid  
52  
53 Chromatography Interfaced with Ion Mobility Mass Spectrometry. *Anal. Chim. Acta* **2018**,

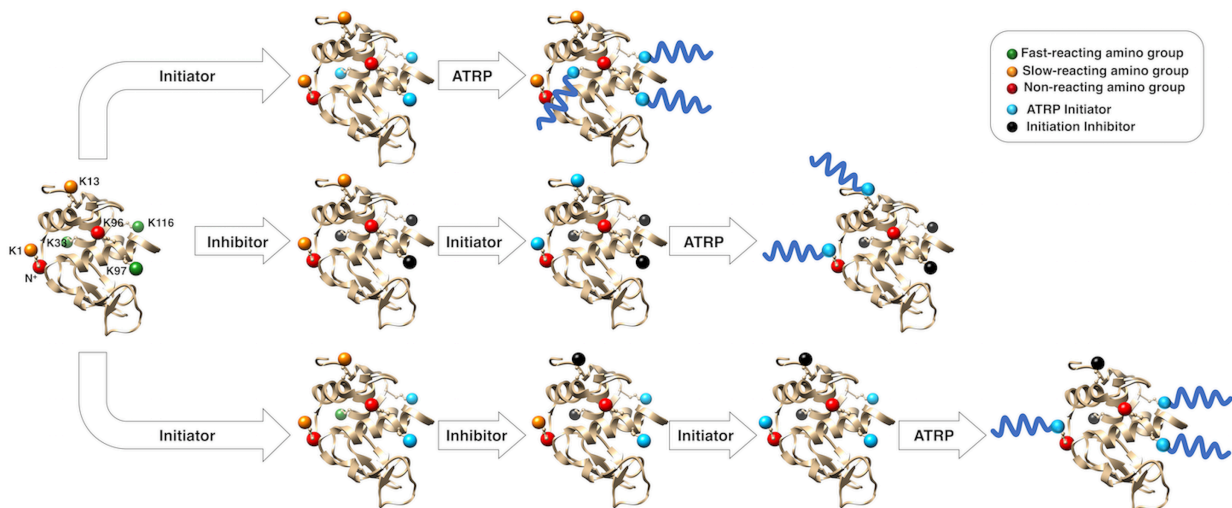
- 1  
2  
3 1004, 58–66.  
4  
5 (24) Wang, G.; De Jong, R. N.; Van Den Bremer, E. T. J.; Parren, P. W. H. I.; Heck, A. J. R.  
6  
7 Enhancing Accuracy in Molecular Weight Determination of Highly Heterogeneously  
8  
9 Glycosylated Proteins by Native Tandem Mass Spectrometry. *Anal. Chem.* **2017**, *89* (9),  
10  
11 4793–4797.  
12  
13  
14 (25) Carmali, S.; Murata, H.; Cummings, C.; Matyjaszewski, K.; Russell, A. J. Polymer-Based  
15  
16 Protein Engineering: Synthesis and Characterization of Armored, High Graft Density  
17  
18 Polymer–Protein Conjugates. In *Methods in Enzymology*; 2017; Vol. 590, pp 347–380.  
19  
20  
21 (26) Peeler, J. C.; Woodman, B. F.; Averick, S.; Miyake-Stoner, S. J.; Stokes, A. L.; Hess, K.  
22  
23 R.; Matyjaszewski, K.; Mehl, R. A. Genetically Encoded Initiator for Polymer Growth  
24  
25 from Proteins. *J. Am. Chem. Soc.* **2010**, *132* (39), 13575–13577.  
26  
27  
28 (27) Carmali, S.; Murata, H.; Amemiya, E.; Matyjaszewski, K.; Russell, A. J. Tertiary  
29  
30 Structure-Based Prediction of How ATRP Initiators React with Proteins. *ACS Biomater.*  
31  
32 *Sci. Eng.* **2017**, *3* (9), 2086–2097.  
33  
34  
35 (28) Johnson, L. N. The Structure and Function of Lysozyme. *Science progress*. Science  
36  
37 Reviews 2000 Ltd. 1966, pp 367–385.  
38  
39  
40 (29) Li, H.; Bapat, A. P.; Li, M.; Sumerlin, B. S. Protein Conjugation of Thermoresponsive  
41  
42 Amine-Reactive Polymers Prepared by RAFT. *Polym. Chem.* **2011**, *2* (2), 323–327.  
43  
44  
45 (30) Lucius, M.; Falatach, R.; McGlone, C.; Makaroff, K.; Danielson, A.; Williams, C.; Nix, J.  
46  
47 C.; Konkolewicz, D.; Page, R. C.; Berberich, J. A. Investigating the Impact of Polymer  
48  
49 Functional Groups on the Stability and Activity of Lysozyme-Polymer Conjugates.  
50  
51 *Biomacromolecules* **2016**, *17* (3), 1123–1134.  
52  
53  
54 (31) Murata, H.; Carmali, S.; Baker, S. L.; Matyjaszewski, K.; Russell, A. J. Solid-Phase  
55  
56  
57  
58  
59  
60

- 1  
2  
3 Synthesis of Protein-Polymers on Reversible Immobilization Supports. *Nat. Commun.*  
4  
5 **2018**, *9* (1), 845.  
6  
7  
8 (32) Smolelis, A. N.; Hartsell, S. E. The Determination of Lysozyme. *J. Bacteriol.* **1949**, *58*  
9  
10 (6), 731–726.  
11  
12 (33) Murata, H.; Cummings, C. S.; Koepsel, R. R.; Russell, A. J. Rational Tailoring of  
13  
14 Substrate and Inhibitor Affinity via ATRP Polymer-Based Protein Engineering.  
15  
16 *Biomacromolecules* **2014**, *15* (7), 2817–2823.  
17  
18  
19 (34) Canfield, R. E. The Amino Acid Sequence of Egg White Lysozyme. *J. Biol. Chem.* **1963**,  
20  
21 *228* (8), 2698–2707.  
22  
23  
24 (35) Browne, W.; North, A.; Phillips, D.; Brew, K.; Vanaman, T.; Hill, R. A Possible Three-  
25  
26 Dimensional Structure of Bovine Alpha-Lactalbumin Based on That of Hen's Egg-White  
27  
28 Lysozyme. *J. Mol. Biol.* **1969**, *42* (1), 65–86.  
29  
30  
31 (36) Suckau, D.; Mak, M.; Przybylski, M. Protein Surface Topology-Probing by Selective  
32  
33 Chemical Modification and Mass Spectrometric Peptide Mapping. *Proc. Natl. Acad. Sci.*  
34  
35 *U. S. A.* **1992**, *89* (12), 5630–5634.  
36  
37  
38 (37) da Silva Freitas, D.; Abrahão-Neto, J. Biochemical and Biophysical Characterization of  
39  
40 Lysozyme Modified by PEGylation. *Int. J. Pharm.* **2010**, *392* (1–2), 111–117.  
41  
42  
43 (38) Lee, H.; Park, T. G. A Novel Method for Identifying PEGylation Sites of Protein Using  
44  
45 Biotinylated PEG Derivatives. *J. Pharm. Sci.* **2003**, *92* (1), 97–103.  
46  
47  
48 (39) Foser, S.; Schacher, A.; Weyer, K. A.; Brugger, D.; Dietel, E.; Marti, S.; Schreitmüller, T.  
49  
50 Isolation, Structural Characterization, and Antiviral Activity of Positional Isomers of  
51  
52 Monopegylated Interferon  $\alpha$ -2a (PEGASYS). *Protein Expr. Purif.* **2003**, *30* (1), 78–87.  
53  
54  
55 (40) Wang, Y.-S.; Youngster, S.; Grace, M.; Bausch, J.; Bordens, R.; Wyss, D. F. Structural  
56  
57  
58  
59  
60

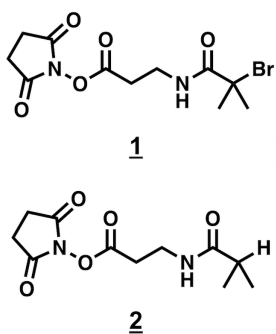
- 1  
2  
3 and Biological Characterization of PEGylated Recombinant Inteferon Alpha-2b and Its  
4  
5 Therapeutic Implications. *Adv. Drug Deliv. Rev.* **2002**, *54*, 547–570.  
6  
7  
8 (41) Finn, R. F. PEGylation of Human Growth Hormone: Strategies and Properties. In  
9  
10 *PEGylated Protein Drugs: Basic Science and Clinical Applications*; Birkhauser Verlag:  
11  
12 Basel, 2009; pp 187–203.  
13  
14 (42) Wang, G.; Hu, J.; Gao, W. Tuning the Molecular Size of Site-Specific Interferon-Polymer  
15  
16 Conjugate for Optimized Antitumor Efficacy. *Sci. China Mater.* **2017**, *60* (6), 563–570.  
17  
18 (43) Liu, M.; Johansen, P.; Zabel, F.; Leroux, J. C.; Gauthier, M. A. Semi-Permeable Coatings  
19  
20 Fabricated from Comb-Polymers Efficiently Protect Proteins in Vivo. *Nat. Commun.*  
21  
22 **2014**, *5* (5526), 1–8.  
23  
24 (44) Chen, X.; Muthoosamy, K.; Pfisterer, A.; Neumann, B.; Weil, T. Site-Selective Lysine  
25  
26 Modification of Native Proteins and Peptides via Kinetically Controlled Labeling.  
27  
28 *Bioconjug. Chem.* **2012**, *23* (3), 500–508.  
29  
30 (45) Parmar, A. S.; Muschol, M. Hydration and Hydrodynamic Interactions of Lysozyme:  
31  
32 Effects of Chaotropic versus Kosmotropic Ions. *Biophys. J.* **2009**, *97* (2), 590–598.  
33  
34 (46) Price, J. A. R.; Pethig, R. Surface Charge Measurements on *Micrococcus Lysodeikticus*  
35  
36 and the Catalytic Implications for Lysozyme. *Biochim. Biophys. Acta* **1986**, *889*, 128–135.  
37  
38 (47) Pethig, R.; Price, J. A. R. The Influence of Electrostatic Interactions on the Activity of  
39  
40 Lysozyme. *Int. J. Quantum Chem.* **1986**, *30* (13 S), 39–51.  
41  
42  
43  
44  
45  
46  
47  
48  
49  
50  
51  
52  
53  
54  
55  
56  
57  
58  
59  
60

## TABLE OF CONTENTS GRAPHIC





a.



b.

